This is a peer-reviewed, accepted author manuscript of the following research article: Jawad, M., Jahanzaib, M., Ali, M. A., Farooq, M. U., Mufti, N. A., Pruncu, C. I., Hussain, S., & Wasim, A. (Accepted/In press). Revealing the microstructure and mechanical attributes of pre-heated conditions for Gas Tungsten Arc Welded AISI 1045 steel joints. *International Journal of Pressure Vessels and Piping*.

Revealing the microstructure and mechanical attributes of pre-heated conditions for Gas Tungsten Arc Welded AISI 1045 steel joints

Muhammad Jawad[1], Mirza Jahanzaib[1], Muhammad Asad Ali[1,2,*], Muhammad Umar Farooq[2,*], Nadeem Ahmad Mufti[2], Catalin I. Pruncu[3,4,*], Salman Hussain[1], Ahmad Wasim[1]

[1]Department of Industrial Engineering, University of Engineering and Technology, Taxila 47080, Pakistan. engr.jawad@uettaxila.edu.pk (M. Jawad) jahan.zaib@uettaxila.edu.pk (M. Jahanzaib); salman.hussain@uettaxila.edu.pk (S. Hussain); wasim.ahmad@uettaxila.edu.pk (A. Wasim)

[2]Department of Industrial and Manufacturing Engineering, University of Engineering and Technology, Lahore 54890, Pakistan. namufti@uet.edu.pk (N.A. Mufti)

[3]Department of Mechanical Engineering, Imperial College London, Exhibition Rd., SW7 2AZ, London, UK

[4]Design, Manufacturing & Engineering Management, University of Strathclyde, Glasgow, G1 1XJ, Scotland, UK

*Corresponding authors: c.pruncu@imperial.ac.uk ; Catalin.pruncu@strath.ac.uk (C.I. Pruncu); asad.ali@uet.edu.pk (M.A. Ali); Umarmuf0@gmail.com (M.U. Farooq)

Abstract

Gas tungsten arc welding (GTAW) is considered a well-established process in the manufacturing industry. Despite, certain challenges associated with high hardness of heat affected zone and cold cracking susceptibility of joints, are the main barriers for this process to be implemented successfully within high integrity structure. By using a combined procedure of experiments and modelling (response surface methodology (RSM) and multi-objective optimization: multi-objective genetic algorithm (MOGA)) allows obtaining good enhancement over uniform heating, cooling and the heat-affected zone which enable major progress in obtaining high quality welded parts. Therefore, this research study combines the experiments and modelling in a systematic manner considering for the first type the pre-heated treatment and without- pre-heating conditions of GTAW manufacturing. It leads to optimizing the process parameters of GTAW when manufacturing AISI 1045 medium carbon steel. The effects of critical parameters i.e. welding current: W_C, welding speed: W_S, and gas flow rate: G_{FR} on the mechanical properties (ultimate tensile strength (UTS) and hardness) were investigated and evaluated against the microstructure of weld fracture. The multi-objective genetic algorithm corroborated with experimental observation enables to obtain a maximum UTS of approx. 625 MPa and hardness of 80.19 HRB for preheat condition. The results highlight an improvement in UTS of 0.2% to 6.7% and a decrease in hardness of 0.1% to 21.5% by implementing the preheating condition.

Keywords: Gas tungsten arc welding; fractography; response surface methodology; genetic algorithm; ultimate tensile strength; hardness.

Introduction

Recently, medium carbon steels, specifically, AISI 1045 have gained attention because of their properties including high toughness, strength and wear resistance. Therefore, it has been used in several applications containing axels, bolts, connecting rods, spindles, torsion bars, worms, light gears, crankshaft and several other automotive, petroleum and piping products [1].

Manufacturing complex parts using AISI 1045 steel as a single component without joints is a cumbersome task, this raises the need for preparing parts in joints [2]. In the case of joining metals with carbon content above 0.35%, the heat-affected zone of medium carbon steels become fully hardened which results in cold cracking and brittle microstructure that ultimately reduces the weld strength [3]. For these materials (having carbon contents more than 0.35%) proper pre-heating before welding is necessary to avoid cold cracking and brittle microstructure [4]. Welding of these materials has been effectively carried out through gas metal arc welding (GMAW), shielded metal arc welding (SMAW), submerged arc welding (SAW) but for the above-mentioned applications, gas tungsten arc welding (GTAW) is an excellent choice [5]. However, GTAW is preferred over GMAW and SMAW because of the optimum product cost due to its embedded properties including better surface quality, strength and reasonable production rate. The annual market share of manufactured parts especially welded pieces crossed $19.53 Billion and is expected to grow up to $27.22 by 2026 [6–8]. The scope of these products is exponentially expanding with the rise in novel industrial requirements such as in the railway industry, the axle is potentially manufactured through arc welding. Moreover, process usage has a prime significance in the automotive industry due to its flexibility and cost-effectiveness.

The high strength and quality of GTAW joints depend upon mechanical properties which are greatly influenced by different process variables for instance; welding current, torch angle, welding speed, gas flow rate and arc voltage [9–13]. Various researchers have been evaluated the impact of process parameters on the mechanical properties (ultimate tensile strength and hardness) of gas tungsten arc welded joints. Welding current and speed were the most prominent parameters that impact the strength and hardness of GTAW A516-Gr70 carbon steel joints [14]. Chuaiphan and Srijaroenpramong [15] studied the influence of welding speed on tensile strength and hardness of AISI 201 stainless steel joints in GTAW. They observed that high tensile strength and hardness were achieved at high welding speed. Choudhury et al. [16] optimized the GTAW parameters by joining mild steel and stainless steel. Maximum ultimate tensile strength (UTS) was achieved at optimum parametric conditions: current of 100 A, gas flow rate of 18 l/min and filler rod diameter of 1.6 mm. Singh et al. [17] found that maximum UTS was attained at the gas flow rate of 5 LPM, current of 40 A and welding speed of 12 m/min. In a study of hot sintered forged AISI 4135 PM steel GTAW joints, it was established that welding speed was the most vital factor for UTS [11]. Rao and Deivanathan [10] reported that the tensile strength of GTA welded 310 Austenitic SS joints was increased by an increment in the welding current up to 125 A and welding defects were reduced. Wang et al. [18] found that improvement in strength was resulted from decreasing the hardness. Fracture features were analyzed which revealed that GTAW joints were ductile. Kumar et al. [19] examined the influence of process variables on mechanical properties of aluminium alloy 6061 joints and found that welding current was the most prompting factor that influenced hardness and % elongation. Liu et al. [20] examined the hardness of GTAW joints of dissimilar Al and Mg alloys. A significant increase in microhardness of Al and Mg fusion zone was found as compared to the base metal. Dendritic structure was found in GTAW of 304 stainless steel (SS) and the hardness of heat affected zone (HAZ) was found less than base metal and weld metal [21]. Simhachalam et al. [22] reported that current was the most influencing parameter for tensile strength of GTA welded 304(18Cr-8 Ni) SS joints. While better hardness was found at higher welding current. A comparison was performed in GTAW and Metal inert gas (MIG)

welding of AISI 1020 low carbon steel joints. It was infrared that % contribution of welding current was more than other parameters and hardness was increased with increase in welding current [23]. In another study on GTAW of AISI 1019 low carbon steel plates, it was observed that voltage and current were significant parameters for tensile strength, whereas welding speed was significant factor for hardness [24]. Takhti et al. [25] studied the microstructural and mechanical properties of aluminum alloy A356 by using GTAW. It was concluded that fracture did not occur at fusion zone for all specimen revealed that GTAW joints have high strength than the parent metal. Kishore et al. [26] reported that defects like LOP, blow holes and cracks in AISI 1040 steel joints were reduced by increasing the current up to 180 A for MIG welding and 80 A for GTAW.

The literature review reveals that GTAW process parameters for instance; welding speed, welding current and gas flow rate significantly affects the mechanical properties of welded joints [16,19,27–34]. Figure 1 present details of the literature review on GTAW of different materials which can help to detect a suitable tool for GTAW assessment. It can be observed, various statistical and modelling techniques such as the Taguchi method, factorial design, genetic algorithm, fuzzy logic, response surface methodology and artificial neural network have been employed to model and optimize the responses by researchers [16,19,28,33]. Primarily, figure 1 shows the literature summary including different optimization techniques, output responses, and workpiece materials used in the GTAW process. The highlighted area in the figure represents the RSM technique which is selected in the current study for optimization. Some of them are fast but very expensive, they require numerous parameters and high skills from engineers, and others seem only intuitive. It was concluded that response surface methodology (RSM) can enable a systematic evaluation which was not fully explored in the past for the GTAW. The significance of RSM is related to its cost-effective in predicting with accuracy the best mechanical properties though generating an optimal combination of input process parameters [35]. Moreover, to optimize the parameters, one of the advanced metaheuristics namely multi-objective genetic algorithm (MO-GA) is employed to explore optimized settings under both conditions.

In this research, we have integrated systematically the experimental determination and numerical approximation (RSM) and multi-objective optimization (MO-GA) to detect the effects of critical parameters involved during GTAW. It allows generating the best manufacturing condition which leads to maximum mechanical properties for joined parts. To further improve the state of the art we have investigated the effect of pre-heating treatment which have a substantial impact on improving the mechanical properties of the weld. This is because it plays a vital role in slowing down the cooling rate, promotes fusion in welding, hence improves the quality and strength of GTA weld [36,37]. The systematic evaluation through RSM and MO-GA combined with novel pre-heating treatment enabled obtaining a superior GTAW process that finally leads to create highly integrity welded structures made of AISI 1045 medium carbon steel for the automotive industry.

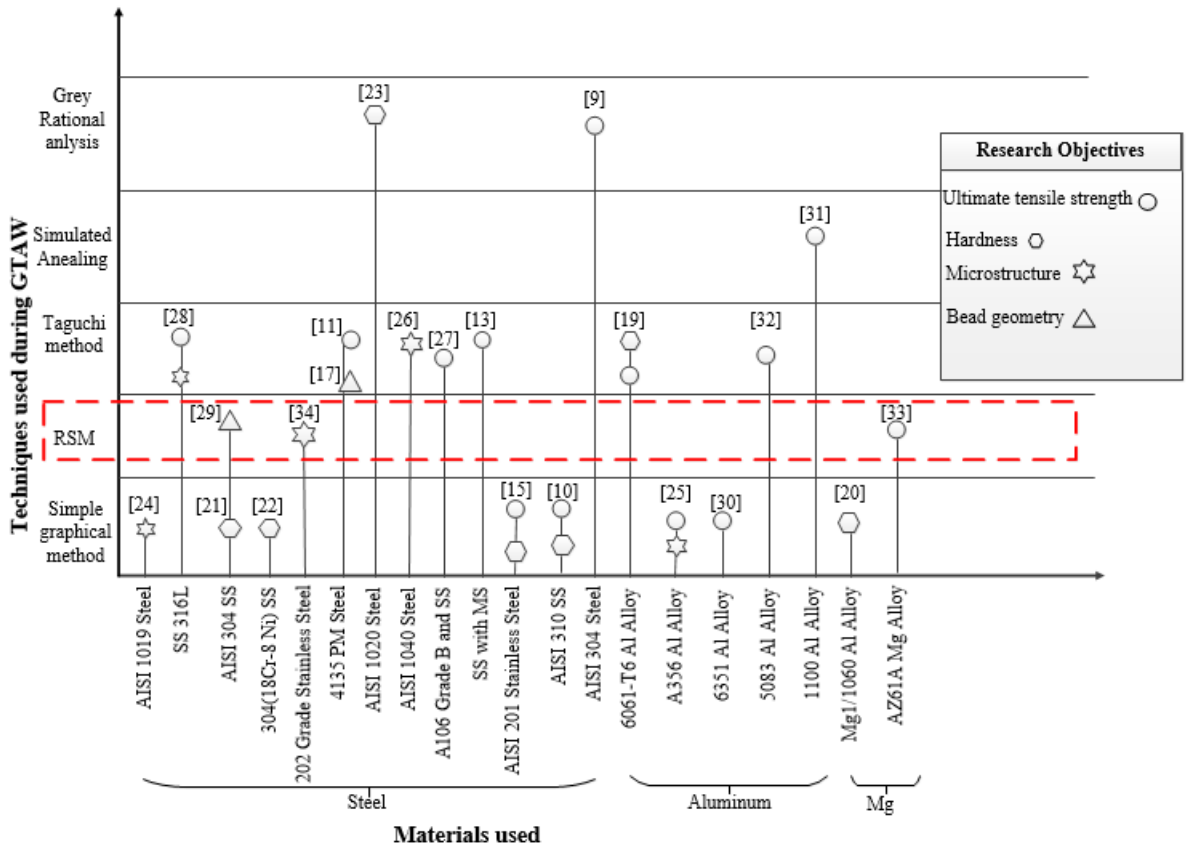

Figure 1. Brief literature on GTAW materials and techniques used

Experimental details

This section briefly describes the experimental procedure, chemical composition of the material, sample preparation and measurement of responses. Gas tungsten arc welding (GTAW) was carried on two plates of AISI 1045 medium carbon steel having dimensions of 100 mm × 80 mm × 4 mm. Chemical composition is validated through spark emission spectroscopy with the composition received from the manufacturer. In addition, the mechanical properties of the material are tested through tensile and hardness testing machines before experimentation and are provided in Table 1. GTAW inverter (LINCOLN ELECTRIC-V270-T) with amperage range 5 to 270 A was used to join the plates. Argon gas was applied for shielding the weld joints from atmospheric gases. Prior to welding, a V-groove has been made on the joining side of base metal for the proper fusion of filler metal. The angle of the welding torch with base metal was kept at 75º. Pre-heating of samples was performed in an electric furnace at 250°C temperature. The K-type thermocouple was used to ensure the preheating temperature as shown in figure 2. However, they are not used for continuous monitoring in the process. Preheating temperature is estimated by calculating the carbon equivalent (CE) of AISI 1045 medium steel, from equations (1) and (2) [8, 34, 35].

$$CE = C + \frac{Mn+Mo}{10} + \frac{Cr+Cu}{20} + \frac{Ni}{40}\ (\%) \qquad (1)$$

and

$$Preheating\ temperature = 750\ °C\ \times CE - 150\ °C \qquad (2)$$

The gas flow rate value was controlled by a flow meter, whereas the welding current was controlled by the GTAW inverter. To obtain a uniform welding speed, a microcontroller-based separate feed-controlled mechanism embedded with Arduino was specially designed. Fine pointed tungsten electrode shape was ensured before each welding. ER 70S mild steel filler wire having 1.6 mm diameter as per American welding society (AWS) classification was used for fusion of metals. The welding mechanism was equipped with wire feeders, feeding wires simultaneously to the melt pool with a constant wire feed of 2 m/min for all experiments. The overall methodology of the study has been presented in figure 2. The schematic illustration of the GTAW process is presented in figure 3.

Table 1. Chemical composition and Mechanical Properties of AISI 1045

Chemical Composition									Mechanical properties	
Elements	C	Si	Mn	S	P	Ni	Cu	Fe	UTS (MPa)	Hardness (HB)
Wt. %	0.46	0.23	0.84	0.003	0.011	0.01	0.01	Balance	575	73

The mechanical attributes of GTA welded AISI 1045 joints were evaluated through UTS and hardness. Samples for the UTS test and hardness were extracted from the welded samples. Tensile samples were made as per ASTM standards E8M-08 [40]. A total number of 38 tensile specimens were extracted (19 preheated and 19 without preheating) as presented in figure 2. The tensile test was performed at a strain rate of 1 s^{-1} using material testing systems (810-MTS). Under each experimental condition, three samples were tested and the final value of UTS was obtained by taking the average to minimize the error. Tensile specimens for pre-heating and without pre-heating are shown in figure 2. Hardness test was carried out on Universal hardness tester by selecting Rockwell hardness scale ‘B’ with 90 kg load. Three readings of hardness were taken on the weld area of each sample and the final value of hardness was obtained by taking an average. For fractography, scanning electron microscopy (SEM) was used. The images were observed at 20 to 200 µm resolution. SEM images were separately taken for pre-heating samples and without preheating samples.

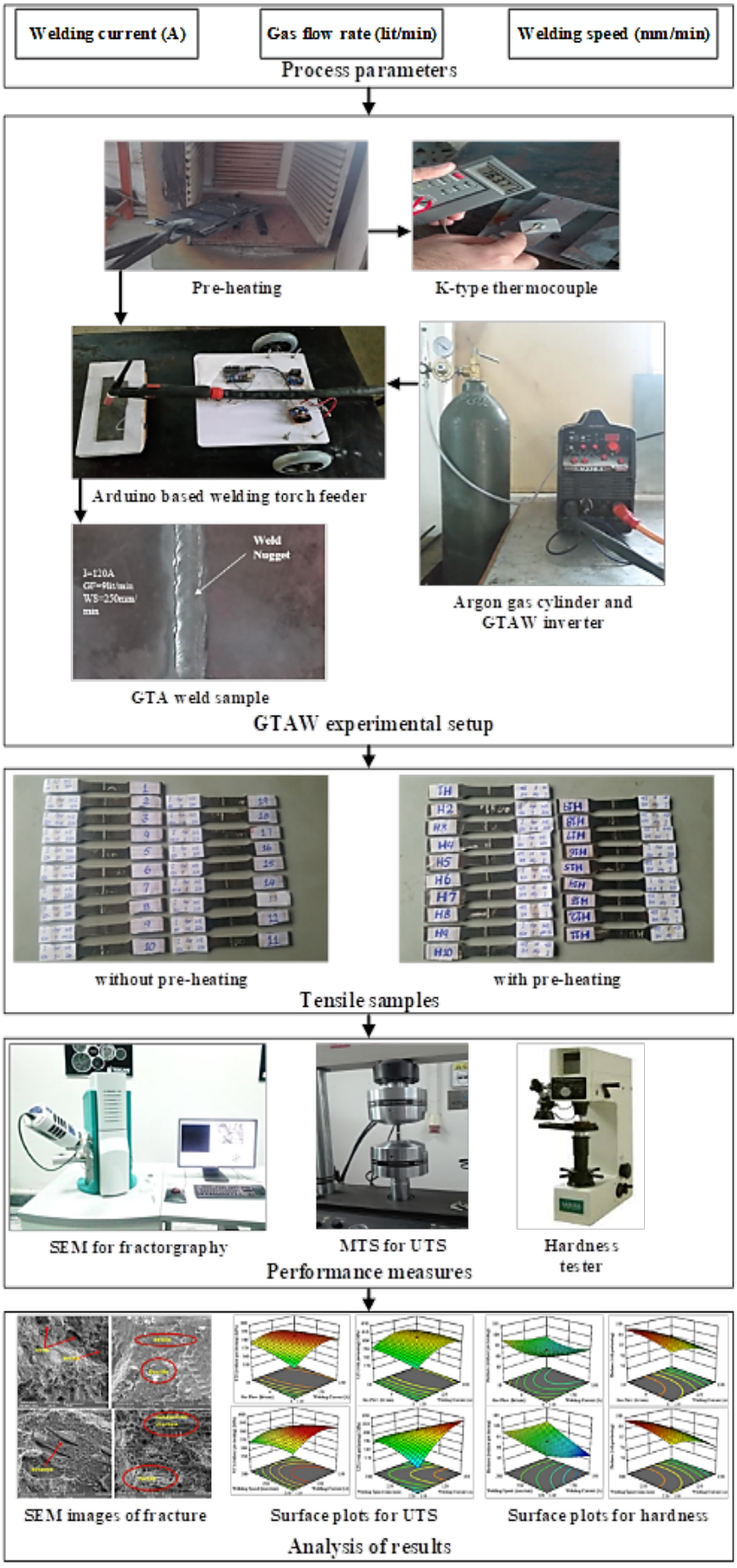

Figure 2. Experimental methodology

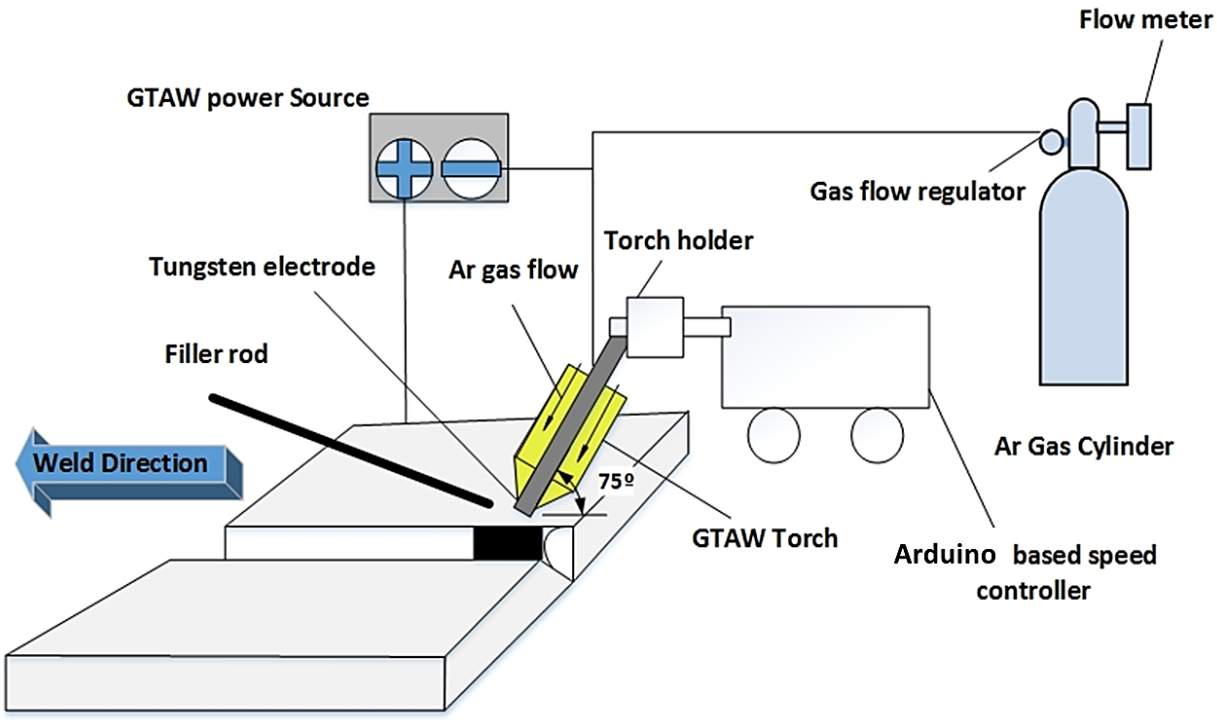

Figure 3. Schematic illustration of the GTAW process

Experimental design

The important welding parameters and ranges have been identified from the literature review. Three gas tungsten arc welding (GTAW) parameters such as welding current (W_C), gas flow rate (G_{FR}) and welding speed (W_S) were selected in this study due to their significant effect on mechanical properties [14, 16, 23, 37, 38]. Based on trial runs, the maximum and minimum values of parameters were selected in such a way that uniform and defect-free weld joints obtained. Parameters and their ranges are shown in Table 2. Response surface methodology (RSM) has been used to analyze and model the responses (as recommended in literature [35]). GTAW of AISI 1045 joints were performed on two different temperature conditions: without pre-heating and with pre-heating. Overall, 38 experiments (19 with pre-heating and 19 without pre-heating) were performed according to RSM central composite design (CCD) from equation (3).

$$Number\ of\ experiments = 2^n + 2(n) + n_c \quad (3)$$

Where, n = number of factors, n_c = number of center points. Center point represents the replications of experimental runs. To estimate the experimental error or to affirm the accuracy in design of experiments, the rule of thumb is to have 3 to 5 center points [42]. In the current study, the number of center points selected in the design was 5 and the number of factors were 3. The α points, shown in Table 2, describes the rotatability of response surface design. RSM is a design of experiment as well as an optimization technique and location of optimum value is unknown before experimentation, therefore, the design that provides equal precision of estimation in all directions (positive and negative) must be selected [42]. In the current study, the rotatable design is selected on the basis of these α points and experiments are performed on these points accordingly.

Table 2. Welding parameters and their ranges

Process parameters	Unit	Levels				
		-α points	Low	Middle	High	+α points
Welding current	A	103.18	110	120	130	136.81
Gas flow rate	lit/min	7.31	8	9	10	10.68
Welding speed	mm/min	199.54	220	250	280	300.45

Results and discussion

Development of mathematical models

Mathematical models are developed to predict the responses including ultimate tensile strength and hardness by using statistical software. Analysis of variance (ANOVA) has been carried out at 95% confidence interval has shown in Table 3 is used to check the significance of parameters and adequacy of models [35].

Ultimate tensile strength

Fit summary suggested that quadratic models are appropriate for ultimate tensile strength in the case of both pre-heating and without pre-heating joints. Analysis of variance (ANOVA) results shows that the main effects W_C, G_{FR} and W_S; interaction and quadratic effects of all parameters were significant in case of without pre-heating. Main effects W_C, G_{FR} and W_S; interaction effect of ($W_C \times G_{FR}$) and ($W_C \times W_S$); and quadratic effects of all parameters were significant in the case of pre-heating joints. P-value is less the 0.05 which indicate the significance of the model and parameters. The values of R^2, adjusted R^2 and predicted R^2 are closer to unity for both cases (which is recommended for better reliability and predictability [43]); pre-heating and without pre-heating which show the adequacy of models. Mathematical models for predicting the UTS under pre-heating and without pre-heating conditions are presented in equations (4) and (5) respectively.

$$UTS\ (with\ pre-heating) = -3106.0877 + 36.7829W_C + 54.7619G_{FR} + 10.0154W_S - 0.1625W_C \times G_{FR} - 0.0504W_C \times W_S - 0.0208G_{FR} \times W_S - 0.0919W_C^2 - 1.5932G_{FR}^2 - 0.0081W_S^2 \quad (4)$$

$$UTS\ (without\ pre-heating) = -1894.9817 + 25.1102W_C + 110.9506G_{FR} + 3.7557W_S - 0.4000W_C \times G_{FR} - 0.0083W_C \times W_S - 0.1083G_{FR} \times W_S - 0.0793W_C^2 - 1.9258G_{FR}^2 - 0.0039W_S^2 \quad (5)$$

Hardness

Fit summary suggested that quadratic models are appropriate for hardness in the case of both pre-heating and without pre-heating joints. ANOVA results revealed that main effects W_C and W_S; interaction effects of ($W_C \times W_S$), ($G_{FR} \times W_S$); and quadratic effects W_C^2 and G_{FR}^2 were significant model terms associated with hardness for without pre-heating joints. W_C, G_{FR}, W_S, ($W_C \times G_{FR}$), ($G_{FR} \times W_S$) and all quadratic effects were significant model terms in the case of pre-heating joints. The values of R^2, adjusted R^2 and predicted R^2 are closer to unity for both cases; pre-heating and without pre-heating. Mathematical equations for predicting the models for hardness under pre-heated and without pre-heated conditions are presented in equations (6) and (7), respectively.

$$Hardness\ (with\ pre-heating) = -980.1947 + 9.1843W_C + 63.7965G_{FR} + 2.0907W_S - 0.1318W_C \times G_{FR} - 0.0034W_C \times W_S - 0.0718G_{FR} \times W_S - 0.0326W_C^2 - 1.5823G_{FR}^2 - 0.0019W_S^2 \quad (6)$$

$$Hardness\ (without\ pre-heating) = +372.1044 - 3.1283W_C - 18.7532G_{FR} - 0.0904W_S - 0.0175W_C \times G_{FR} + 0.0055W_C \times W_S - 0.0608G_{FR} \times W_S + 0.0071W_C^2 + 2.0169G_{FR}^2 + 0.0002W_S^2 \quad (7)$$

Table 3. ANOVA results for UTS and hardness

UTS (without pre-heating)						**UTS (with pre-heating)**					
Source	Sum of squares	Df	Mean square	F value	p-value	Source	Sum of squares	Df	Mean Square	F value	p-value
Model	1787.22	9	198.58	85.57	< 0.0001	Model	4866.721	9	540.747	143.962	< 0.0001
W_C	196.96	1	196.96	84.87	< 0.0001	W_C	575.266	1	575.265	153.1526	< 0.0001
G_{FR}	19.72	1	19.72	8.50	0.0172	G_{FR}	25.805	1	25.804	6.870	0.0278
W_S	368.17	1	368.17	158.64	< 0.0001	W_S	767.928	1	767.928	204.445	< 0.0001
$W_C \times G_{FR}$	128.00	1	128.00	55.15	< 0.0001	$W_C \times G_{FR}$	21.125	1	21.125	5.624	0.048
$W_C \times W_S$	50.00	1	50.00	21.54	0.0012	$W_C \times W_S$	1830.125	1	1830.125	487.233	< 0.0001
$G_{FR} \times W_S$	84.50	1	84.50	36.41	0.0002	$G_{FR} \times W_S$	3.125	1	3.125	0.832	0.386
W_C^2	859.75	1	859.75	370.46	< 0.0001	W_C^2	1154.018	1	1154.018	307.234	< 0.0001
G_{FR}^2	50.63	1	50.63	21.82	0.0012	G_{FR}^2	34.652	1	34.652	9.225	0.0141
W_S^2	168.83	1	168.83	72.75	< 0.0001	W_S^2	717.516	1	717.516	191.024	< 0.0001
Residual	20.89	9	2.32			Residual	33.805	9	3.756		
Lack of fit	12.89	5	2.58	1.29	0.4147	Lack of fit	23.005	5	4.601	1.704	0.313
Pure error	8.00	4	2.00			Pure error	10.8	4	2.7		
Cor total	1808.11	18				Cor total	4900.526	18			
Std. Dv.	1.52	R2		0.9884		Std. Dv.	1.939	R^2		0.993	
Mean	577.32	Adjusted R2		0.9769		Mean	600.158	Adjusted R^2		0.986	
C.V. %	0.263	Predicted R2		0.9388		C.V. %	0.323	Predicted R^2		0.961	
Adequate precision		26.08				Adequate precision		34.40			
Hardness (without pre-heting)						**Hardness (with pre-heting)**					
Source	Sum of squares	Df	Mean square	F value	p-value	Source	Sum of squares	Df	Mean Square	F value	p-value
Model	338.310	9	37.590	58.513	< 0.0001	Model	999.066	9	111.007	60.596	< 0.0001
W_C	48.688	1	48.688	75.789	< 0.0001	W_C	670.289	1	670.289	365.894	< 0.0001
G_{FR}	0.813	1	0.813	1.265	0.2898	G_{FR}	31.541	1	31.540	17.217	0.0025
W_S	181.064	1	181.06	281.84	< 0.0001	W_S	57.930	1	57.930	31.622	0.0003
$W_C \times G_{FR}$	0.245	1	0.245	0.381	0.5522	$W_C \times G_{FR}$	13.913	1	13.913	7.595	0.022
$W_C \times W_S$	22.445	1	22.445	34.938	0.0002	$W_C \times W_S$	8.715	1	8.715	4.757	0.057
$G_{FR} \times W_S$	26.645	1	26.645	41.476	0.0001	$G_{FR} \times W_S$	37.195	1	37.195	20.304	0.002
W_C^2	6.858	1	6.858	10.676	0.0097	W_C^2	145.226	1	145.227	79.276	< 0.0001
G_{FR}^2	55.532	1	55.532	86.441	< 0.0001	G_{FR}^2	34.180	1	34.179	18.658	0.002
W_S^2	0.353	1	0.353	0.550	0.477	W_S^2	40.562	1	40.562	22.142	0.0011
Residual	5.782	9	0.642			Residual	16.487	9	1.832		
Lack of fit	5.070	5	1.0140	5.696	0.058	Lack of fit	12.009	5	2.402	2.145	0.240
Pure error	0.712	4	0.178			Pure error	4.478	4	1.111		
Cor total	344.092	18				Cor total	1015.552	18			
Std. Dv.	0.802	R^2		0.983		Std. Dv.	1.353	R^2		0.984	
Mean	95.721	Adjusted R^2		0.966		Mean	87.953	Adjusted R^2		0.968	
C.V. %	0.837	Predicted R^2		0.873		C.V. %	1.5389	Predicted R^2		0.903	
Adequate precision		24.69				Adequate precision		25.69			

Validation of developed models

Confirmation tests were performed to validate the models. The values of variables were selected within the space of a designed matrix. However, these values were different from the central composite design matrix. Three confirmatory experiments have been performed for both cases. Three experimental conditions were; (1) W_C =116 A, G_{FR} = 8.5 lit/min, W_S = 224 mm/min, (2) W_C =126 A, G_{FR} = 9.5 lit/min, W_S = 254 mm/min, and (3) W_C =132 A, G_{FR} = 10.5 lit/min, W_S = 284 mm/min.The result of confirmation tests and percentage error calculated is shown in Table 4. It is cleared from Table 4 that the percentage error between actual and predicted values for UTS and hardness in all cases was less than 3% which proves the adequacy of the model. Moreover, there was a good covenant among experimental and predicted results (figure 4). The percentage error was calculated by using equation (8) [44].

$$\% \, error = \left| \frac{actual \, value - predicted}{predicted \, value} \right| x \, 100 \quad (8)$$

Table 4. Confromatory test results

Run no.	UTS with pre-heating			UTS without pre-heating			Hardness with pre-heating			Hardness without pre-heating		
	Actual	Predicted	Error (%)	Actual	Predicted	Error (%)	Actual	Predicted	Error (%)	Actual	Predicted	Error (%)
1	580	572	1.4	569	566	0.5	83	85	2.4	95.6	94	1.7
2	620	613	1.1	590	587	0.5	95.6	92.7	3.1	94.9	93.6	1.4
3	567	563	0.7	578	574	0.7	79.3	77.9	1.8	101	98.2	2.9

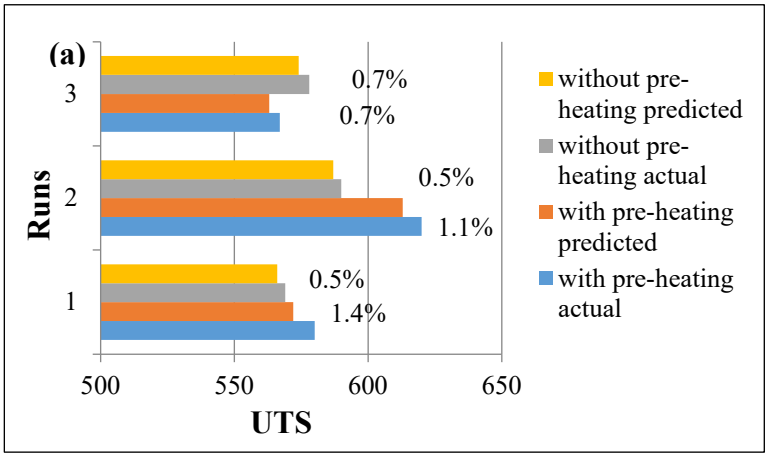

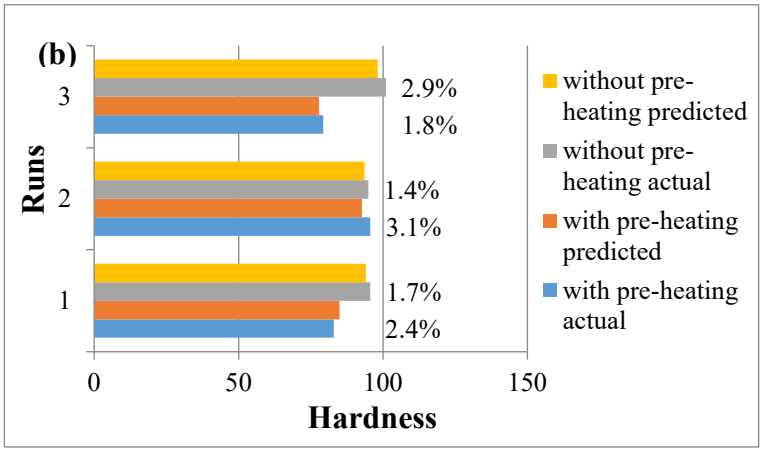

Figure 4. Correlations of Empirical Model (Predicted) and Actual Experimentation with percentage error: (**a**) UTS and (**b**) Hardness

Response surface plot

Effect of input parameters on ultimate tensile strength and hardness for both conditions of pre-heating and without pre-heating has been analysed by 3D surface plots which are briefly described in this section.

Surface plots for ultimate tensile strength

Figure 5(a, b) shows the combined effect of W_C and G_{FR} on ultimate tensile strength for pre-heating and without pre-heating joints. The figure demonstrates that an increase in W_C and G_{FR} causes an increase in the ultimate tensile strength of weld for both conditions. W_C has more effect on UTS as compared to the G_{FR}. Furthermore, UTS increases with an increase in W_C up to a certain level than it decreases at higher values of current. At low current, depth of penetration decreased and lack of fusion occurred but at higher current, the heat input and depth of penetration increases that result in high ultimate tensile strength. For current more than 130 A, the welding defects (spatter and undercut) was observed which agrees well with Kiaee and Aghaie findings [14]. Combine effect of W_S and W_C for without pre-heating and pre-heating joints is shown in figure 6(a, b), respectively. It is evident from the figure that increases in W_C up to middle-level UTS improved, further enhancement in current reduces the ultimate tensile strength. As W_S increases UTS also increases up to a certain limit however at higher W_S slightly decrease in UTS occurred. The effect of welding speed on UTS was in clear agreement with

published research. The authors stated that as the arc travel speed per unit time increases then heat input supplied to weld increases which improve strength but too high W_S reduces the strength due to a decrease in depth of penetration and lack fusion of joining metals [14]. Combine effect of W_S and G_{FR} for without pre-heating and pre-heating joints is shown in figure 7(a, b), respectively. Graphs show that the increase in G_{FR} improves the ultimate tensile strength because high argon gas flow prevents the weld from outer gases and improves its weld properties. Low G_{FR} leads to produce porosities and inclusions in weld. Furthermore, the G_{FR} has a negligible effect on UTS in case of pre-heating. For both conditions, UTS increases with an increase in W_S up to the middle limit than it decreases on further enhancement of W_S.

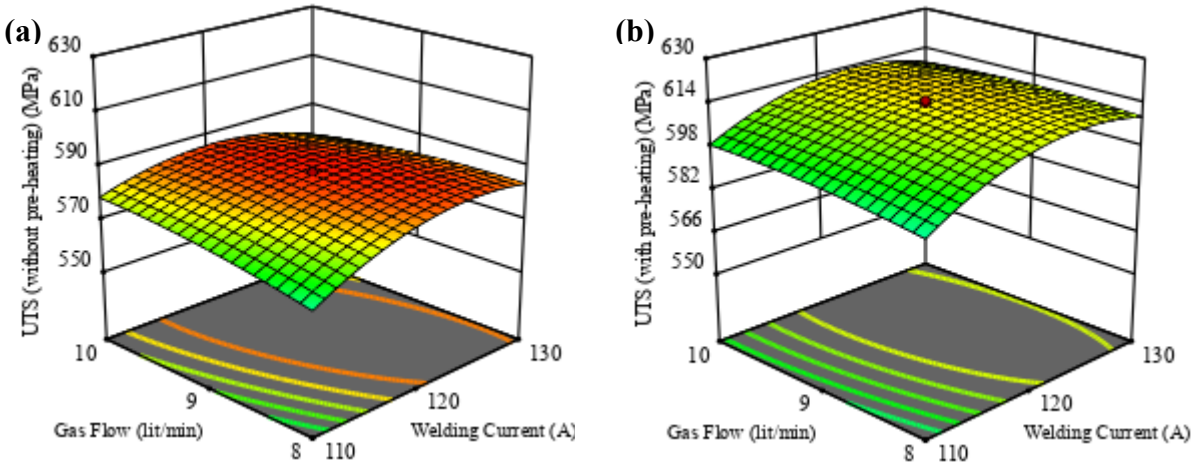

Figure 5. (a) Surface plot welding current vs gas flow rate for UTS without pre-heating, **(b)** Surface plot welding current vs gas flow rate for UTS with pre-heating

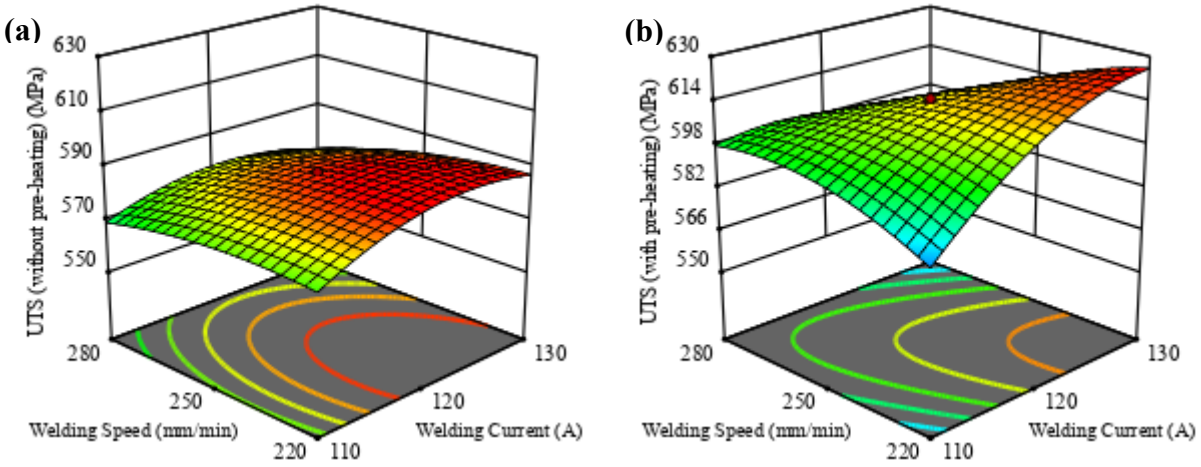

Figure 6. (a) Surface plot welding current vs welding speed for UTS without pre-heating, **(b)** Surface plot welding current vs gas flow rate for UTS with pre-heating

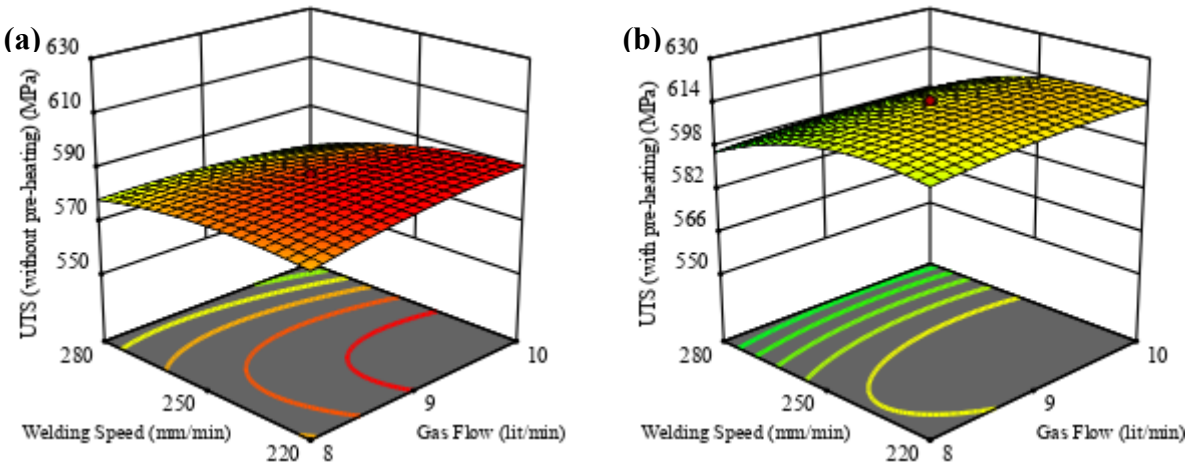

Figure 7. (a) Surface plot welding speed vs gas flow rate for UTS without pre-heating, **(b)** Surface plot welding speed vs gas flow rate for UTS with pre-heating

Surface plots for hardness

Figure 8(a, b) shows the effect of W_C and G_{FR} on hardness without pre-heating and pre-heating joints. It is cleared from figure 8(a) that an increase in G_{FR} and decrease in W_C results increase in hardness of weld without pre-heating. However, W_C has a significant effect on hardness than G_{FR}. But in the case of pre-heating, figure 8(b) shows that an increase in W_C results in decreasing the hardness while G_{FR} has a negligible effect on hardness. At higher welding current, the value of hardness reduced because pre-heating slows down the cooling rate and enhanced the ductility of the weld. Hence, the effect of Wc on hardness in this research was in good agreement with the study of Aglan [45]. Combine effect of W_C and W_S for without pre-heating and with pre-heating joints have been shown in figure 9(a, b), respectively. Almost similar trends are found for both conditions. It is obvious from figures that an increase in W_S and a decrease in current results in increasing hardness of weld. An increase in W_S decreases the heat input and energy transfer into the weld zone that results in a fast cooling rate which ultimately leads to the brittleness of weld, as established in the literature [14]. The effect of W_S and G_{FR} on hardness without pre-heating and pre-heating weld joints is shown in figure 10(a, b), respectively. Figure 10(a) shows that in the case of pre-heating, the hardness increases prominently with an increase in W_S while it decreases with an increase in G_{FR} initially than for further enhancement G_{FR} causes an increase in hardness. For pre-heating joints figure 10(b) indicates that hardness increases sharply with increase in W_S and G_{FR}.

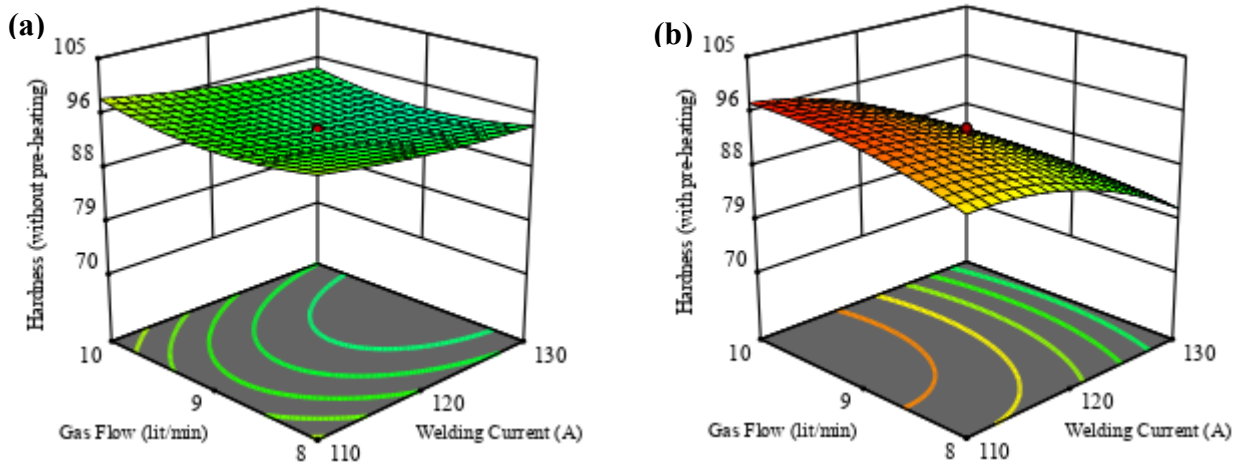

Figure 8. (a) Surface plot welding current vs gas flow rate for hardness without pre-heating, **(b)** Surface plot welding current vs gas flow rate for hardness with pre-heating

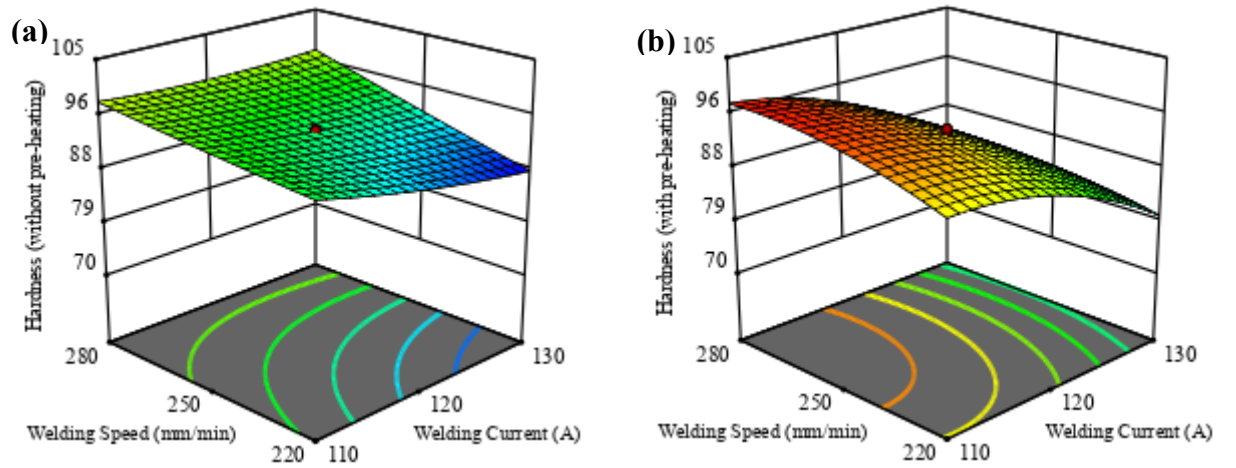

Figure 9. (a) Surface plot welding current vs welding speed for hardness without pre-heating, **(b)** Surface plot welding current vs welding speed for hardness with pre-heating

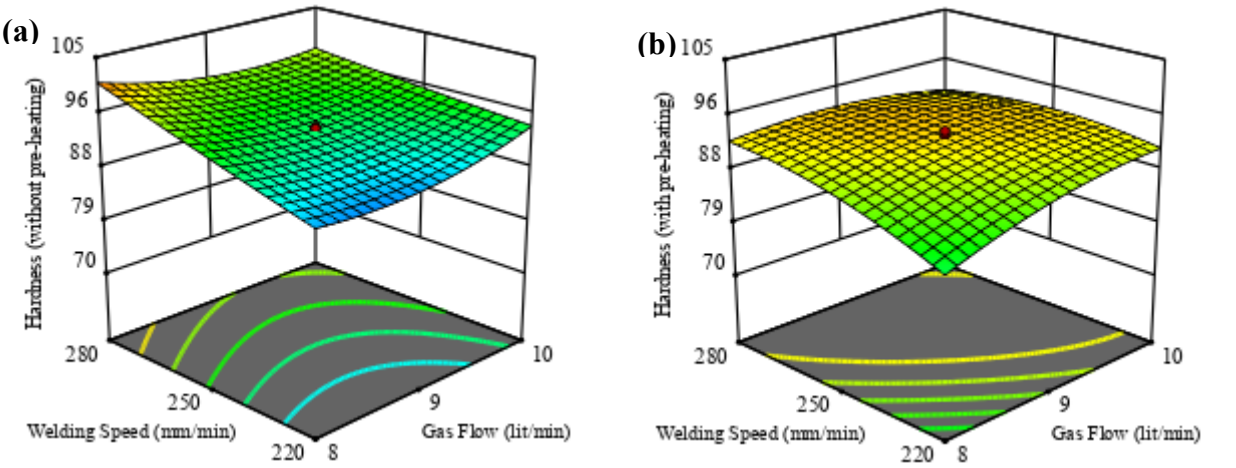

Figure 10. (a) Surface plot welding speed vs gas flow rate for hardness without pre-heating, **(b)** Surface plot welding speed vs gas flow rate for hardness with pre-heating

The samples were cut at a distance of 25 mm from the weld joint for the microstructural examination. A metallurgical microscope at a magnification of 100X was used for the microstructural investigation of the weld joint. Figure 11(a, b) illustrate the microstructural images of weld joint without pre-heating samples on experiments 5 and 14, respectively. Whereas figure 11(c, d) demonstrates characteristics with pre-heating samples on similar

experimental runs. The Fusion zone is formed beside the weld line. Moreover, the heat-affected zone (HAZ) has been generated beyond the fusion zone as indicated in figure 11(a-d). In the case of without pre-heating, as shown in figure 11(a, b) the pearlite and ferrite comprise of dark and bright grains, respectively, are the prominent microstructures of the AISI 1045 steel. Moreover, rapid heating and cooling produce different microstructure in the HAZ region results in a partial martensitic structure [46]. The hardened microstructure of heat affected zone primarily causes a deteriorating phenomenon of welds and cold cracking susceptibility [47]. Similarly, the evidence of martensite results in cracking analogous to the metallurgical notch, as discussed by Anwar et al. [48]. As a result, the martensite-based microstructure increases the hardness. Different cooling rates of the heat-affected zone cause changes in several regions of microstructure, which are determined as root-cause of weld-joint failure [49]. However, in the case of pre-heating samples, a tempered martensitic structure is formed. It is the reason that the hardness of without pre-heated joint is higher than with pre-heated.

The pre-heating of the workpiece supports minimizing the pre-mature crack in weld eventually improving the strength of welded-joint [50]. The prime goal of pre-heating, which is focused on this research, is to control the cooling behavior of welded-joint. This potentially helps in reducing the weld defects such as shrinkage stresses (when compared to without pre-heated welding) and results in a milder cooling rate [51]. The phenomenon of pre-heated settings helps the workpiece's microstructure to be more receptive to the welding process. In general reasonable preheat temperature favors limiting martensite formation and consequent cracking during hardness variations, ultimately improving the weld quality [52]. As a preventive measure, this study determines that AISI 1045 steel should be preheated to decrease the cooling rate after welding to achieve the required quality of the final part. It is cleared from figure 11(a-d) that in case of without pre-heating samples pearlite and martensite prominent present in the HAZ region of weld with cause the lower strength of the weld and increase the hardness.

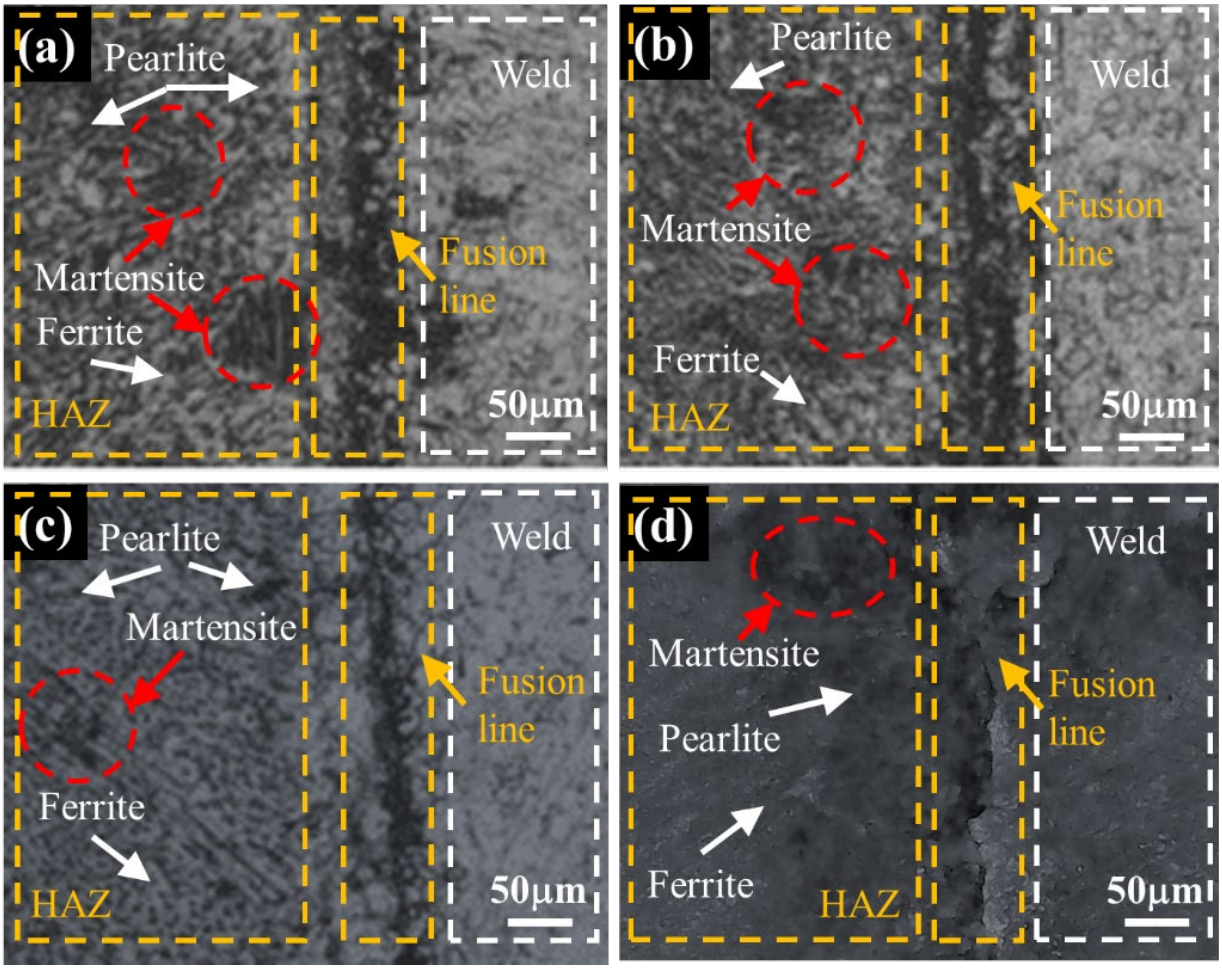

Figure 11. Microstructural images of weld joint for; **(a, b)** without pre-heating, and **(c, d)** with pre-heating

Parametric optimization:

Optimized values of ultimate tensile strength and hardness for pre-heating and without pre-heating joints are obtained from surface plots shown in Table 5. It can be noted from Table 5 that a range of UTS for without pre-heating the joints is between 587 MPa and 590 MPa. This range of UTS is achieved on W_C of 125 A, G_{FR} of 9.2-9.7 lit/min and W_S of 223-225 mm/min. UTS for pre-heating joints is achieved between 614 MPa and 625 MPa which is greater than without pre-heating joints. This high strength range is achieved on the W_C of 123-130 A, G_{FR} of 8.2-9.7 lit/min and W_S of 223-230 mm/min.

To optimize process parameters under conflicting aiding conditions, a multi-objective genetic algorithm (MO-GA) is employed. The tool for the deployment of the algorithm was MATLAB 2020a. The ranges of the process parameters were selected from Table 2. Moreover, the mathematical models of UTS and hardness were used as provided in equations (4-7). The MO-GA attributes selected during deployment were: population of 100, crossover rate of 80%, and mutation rate of 5%. The parameters were adequately tuned before deployment for robust optimization output. The algorithm mimics the behavior of the gene where high crossover ensures maintaining best fits while low mutation helps in not losing genetic traits while flipping [53]. Moreover, the fittest is transferred to the next generation. The Pareto fronts generated during pre-heating and without pre-heating are displayed in figure 12(a,b). The optimized parameters identified are mentioned in Table 5. The parameters 125.83 A W_C, 8.05 lit/min G_{FR},

and 275.13 mm/min W_S have resulted in optimal values 580.31 MPa UTS, and 99.90 HRB hardness in the case of without pre-heating. However, in the case of pre-heating, the parameters 129.75 A W_C, 9.08 lit/min G_{FR}, and 220.08 mm/min W_S produced best results 625.68 MPa UTS, and 80.19 HRB hardness.

Table 5. Optimized values of GTAW parameters with responses

	Response	Process condition	Optimized response values	Parametric values					
				W_C vs G_{FR}		**W_C vs W_S**		**W_S vs G_{FR}**	
				W_C (A)	G_{FR} (lit/min)	W_C (A)	W_S (mm/min)	W_S (mm/min)	G_{FR} (lit/min)
Mono-objective optimization	UTS (MPa)	without pre-heating	587 590 590	123	9	123	223	225	9.7
		with pre-heating	614 625 616	123	8.2	130	223	230	9.7
	Hardness (HRB)	without pre-heating	98 98 100	112	9.8	112	275	275	8.2
		with pre-heating	95 95 93	112	9.2	117	275	265	9.2

	Response	Process condition	Optimized response values	Process parameters		
				W_C (A)	G_{FR} (lit/min)	W_S (mm/min)
MOGA	UTS (MPa) Hardness (HRB)	without pre-heating	580.31 99.90	125.83	8.05	275.13
	UTS (MPa) Hardness (HRB)	with pre-heating	625.68 80.19	129.75	9.08	220.08

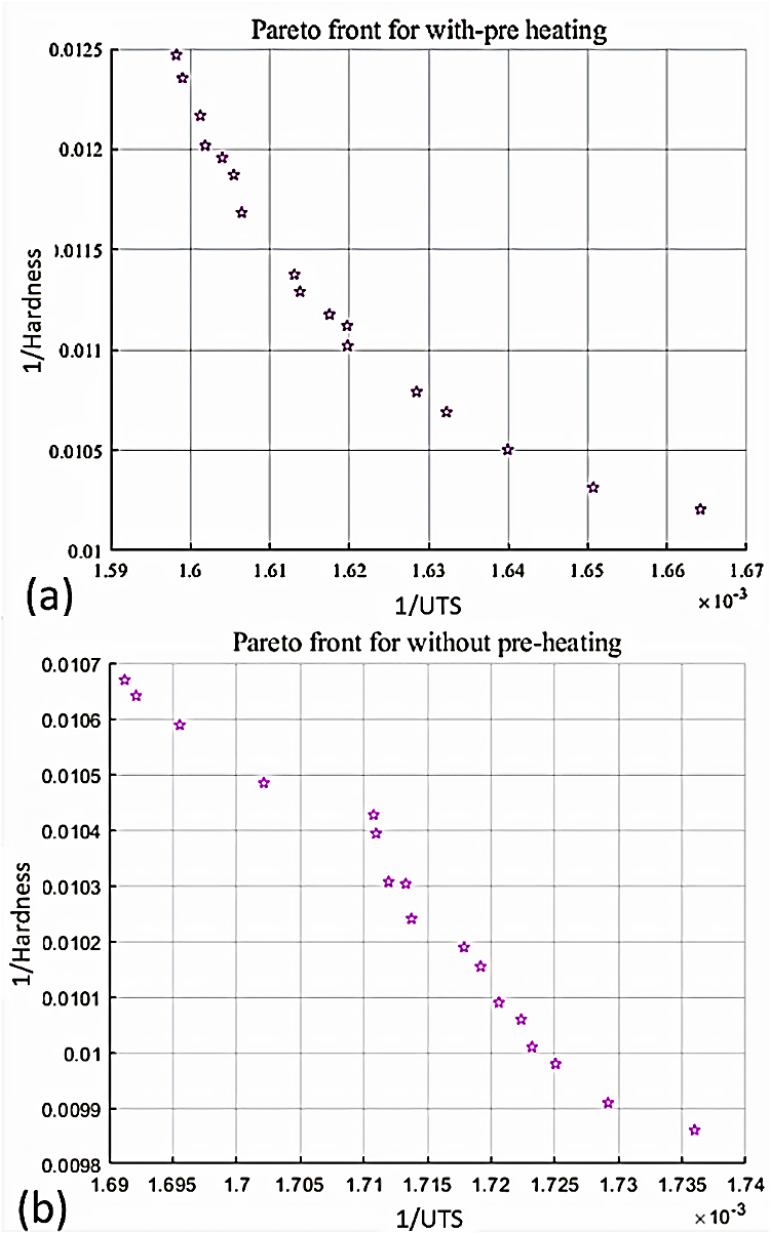

Figure 12. Pareto optimal fronts for **(a)** with pre-heating **(b)** without pre-heating.

Fractography results

The effect of pre-heating on the ultimate tensile strength of GTAW AISI 1045 joints is also analyzed by studying the microstructure of weld fracture with scanning electron microscopy (SEM). The weld fracture of minimum and maximum ultimate tensile strength samples has been selected for both conditions. Figure 13 shows the results of the sample without pre-heating of sample 14. It is clear from the image that a lot of voids and inclusions of oxides from the outer environment is entrapped in the weld due to the fast cooling of the weld and high carbon content so a brittle fracture and minimum UTS (557 MPa) is obtained at low welding current (103 A) and high welding speed (250 mm/min). Figure 14 shows the results of sample 5 without preheating effect. It is obvious from the figure that fewer voids and porosities observed, and the mixture of brittle and ductile fracture obtained. Maximum UTS (590 MPa) is achieved at high current (130 A) and nominal argon gas flow (9 lit/min). Sample 6 results are shown in figure 15. The figure demonstrates that there are inclusions of some oxides due to which it has

low strength, but the pre-heating effect produced cup and cone structure which is ductile and has an ultimate tensile strength (575 MPa). Figure 16 has a high ultimate tensile strength (625 MPa), it is cleared from the figure that there are no inclusions and slag formation. The pre-heating effect slows down the cooling rate which produces purely ductile fracture with cup and cone structure.

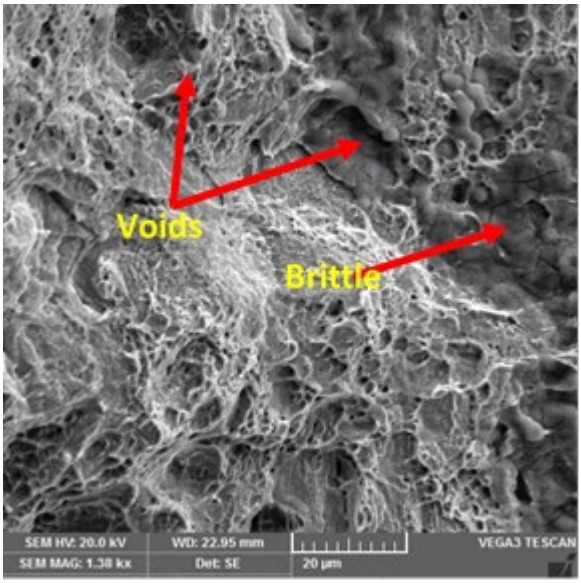

Figure 12. Sample 14 fracture without pre heating

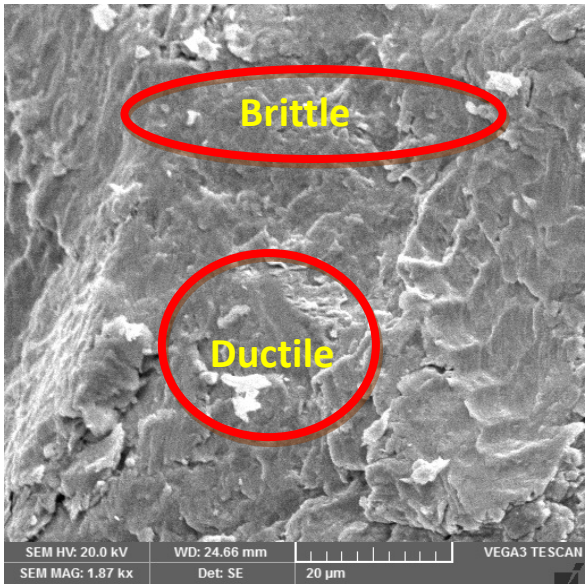

Figure 13. Sample 5 fracture without pre heating

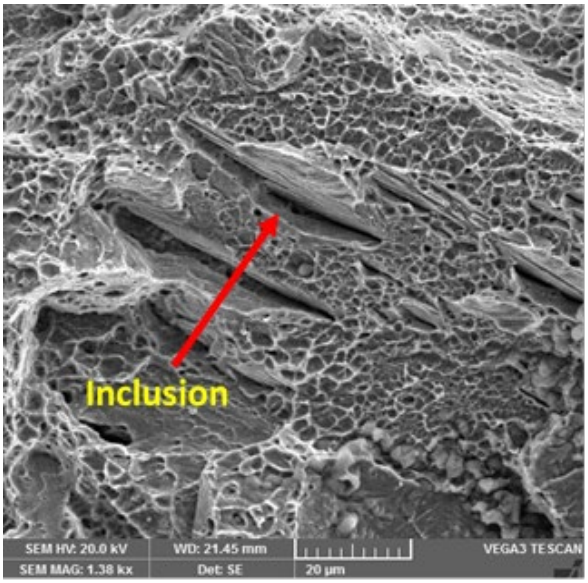

Figure 14. Sample 6 fracture with pre-heating

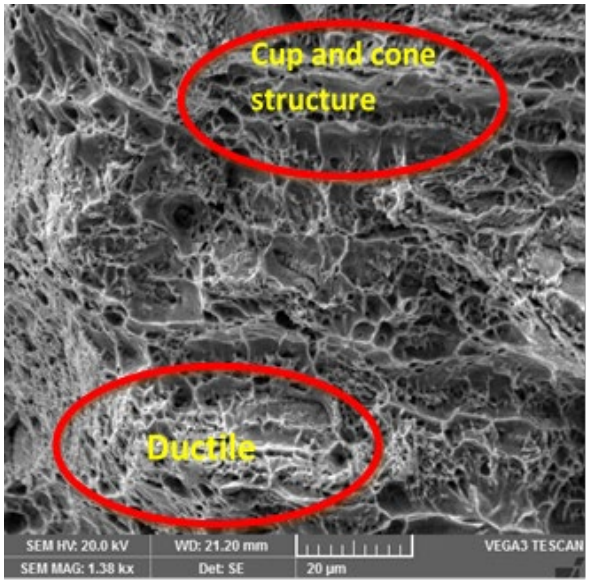

Figure 15. Sample 4 fracture with pre heating

Comparison of pre-heating and not pre-heating GTAW joints

Observed responses of pre-heating and without pre-heating samples for UTS and hardness are compared in figures 17 and 18, respectively. Data for figures represent experimental responses measured. It is cleared from figure 17 that prominent improvement in UTS ranging 0.2% to 6.7% has been observed with pre-heating condition. Figure 18 depicts that a decrease in hardness ranging 0.1% to 21.5% has been found with pre-heating condition.

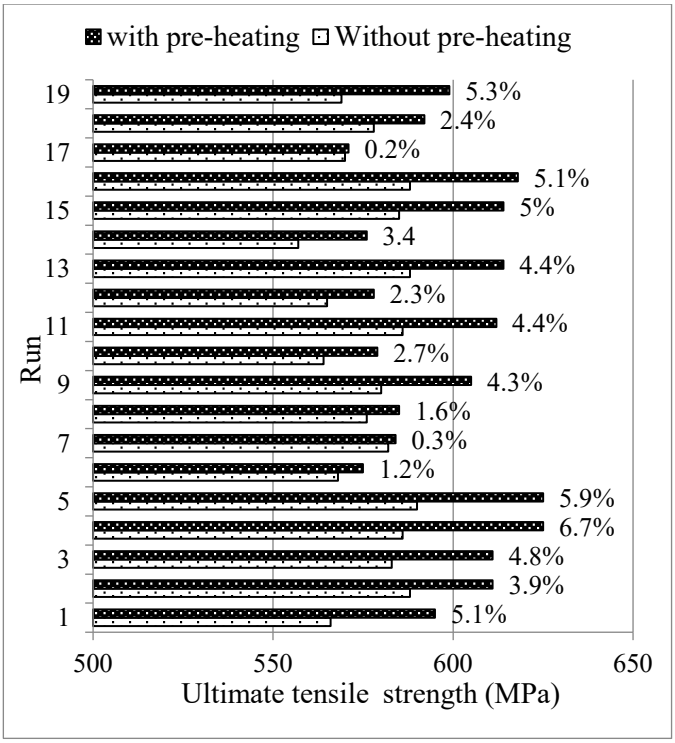

Figure 16. Percentage improvement for UTS

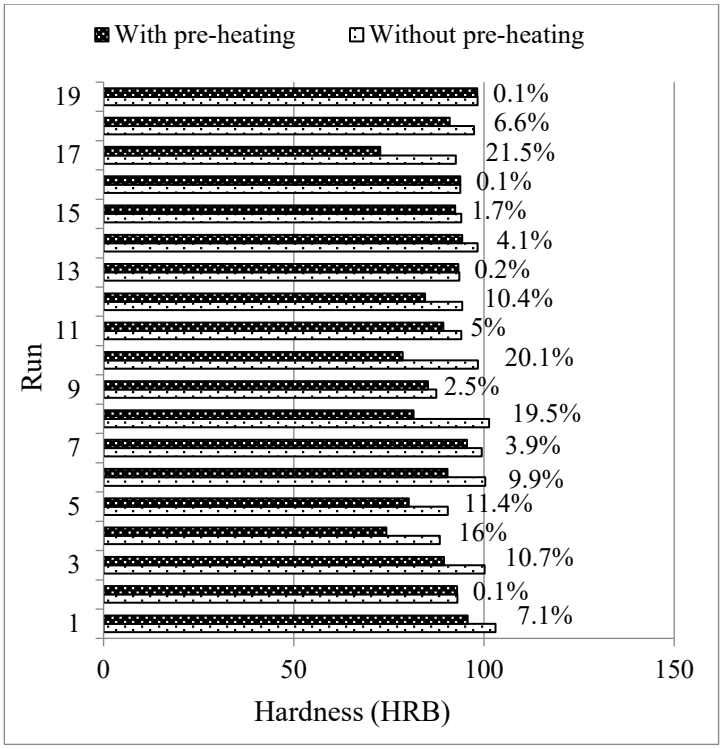

Figure 17. Percentage improvement for hardness

Conclusions

The present investigation was made on gas tungsten arc welding of AISI 1045 medium carbon steel under two conditions: pre-heating and without pre-heating. The effects of W_C, W_S and G_{FR} on mechanical attributes (UTS and hardness) and microstructure of weld fracture surface were analyzed and discussed through the physical phenomenon involved. Through rigorous analyses, the following conclusions are drawn:

- Parametric significance analysis has determined that all input parameters W_C, G_{FR} and W_S are significant parameters for UTS under both conditions (without pre-heating and pre-heating) and hardness under pre-heating.
- An increase in W_C and a decrease in W_S results in improving the UTS. An increase in W_S and decrease in W_C up to a specific value results in increasing the hardness of AISI 1045 GTAW joints.
- Through mono-objective optimization, the maximum value of UTS is found to be 625 MPa and 587 MPa in case of pre-heating and without pre-heating respectively which is higher than the UTS of base metal (575MPa). The maximum value of hardness is achieved to be 95 HRB and 100 HRB with pre-heating and without pre-heating respectively which is higher than the hardness of base metal (73 HRB).
- Multi-objective genetic algorithm resulted in optimized parameters 125.83 A W_C, 8.05 lit/min G_{FR}, and 275.13 mm/min W_S achieved preferred responses 580.31 MPa UTS, and 99.90 HRB hardness in the case of without pre-heating. However, in the case of with pre-heating, the parameters 129.75 A W_C, 9.08 lit/min G_{FR}, and 220.08 mm/min W_S produced the best results 625.68 MPa UTS, and 80.19 HRB hardness.
- Comparative analysis shows prominent improvement in ultimate tensile strength 0.2% to 6.7% while a reasonable decrease in hardness 0.1% to 21.5% under pre-heating condition.

- The fractography results revealed that a large number of inclusions, voids and porosities have been observed and weld fracture was found to be brittle without pre-heating while pure ductile with fewer porosities weld fracture was obtained with pre-heating.

This research confirmed that pre-heating is essential for GTAW of AISI 1045 medium carbon steel to get maximum strength. This research will aid the practitioners to join the complex structures with excellent strength by selecting appropriate input parameters of GTAW without conducting extensive and costly experiments.

References

[1] R.B.P.D.B. Patel and T.M. Patel, A Review on Experimental Investigation of GMAW for AISI 1045 by using Taguchi Method, International Journal for Scientific Research & Development. 1 (2013) 1679–1682.

[2] M. Rafiei, H. Ghayour, H. Mostaan and M.Z. Hosseini, The effect of V addition on microstructure and tribological properties of Fe-Ti-C claddings produced by gas tungsten arc welding, Journal of Materials Processing Technology. 266 (2019) 569–578.

[3] P. Dirisu, S. Ganguly, A. Mehmanparast, F. Martina and S. Williams, Analysis of fracture toughness properties of wire+ arc additive manufactured high strength low alloy structural steel components, Materials Science and Engineering: A. 765 (2019) 138285.

[4] H. Aglan and T. Rahman, Effect of Preheating Temperature and Cooling Rate on the Microstructure Development of Welded Pearlitic Rail Steel, Microscopy and Microanalysis. 26 (2020) 2662–2663.

[5] O.S. Odebiyi, S.M. Adedayo, L.A. Tunji and M.O. Onuorah, A review of weldability of carbon steel in arc-based welding processes, Cogent Engineering. 6 (2019) 1609180.

[6] J.P. Oliveira, T.M. Curado, Z. Zeng, J.G. Lopes, E. Rossinyol, J.M. Park, N. Schell, F.B. Fernandes and H.S. Kim, Gas tungsten arc welding of as-rolled CrMnFeCoNi high entropy alloy, Materials & Design. 189 (2020) 108505.

[7] W. Chuaiphan and L. Srijaroenpramong, Effect of hydrogen in argon shielding gas for welding stainless steel grade SUS 201 by GTA welding process, Journal of Advanced Joining Processes. (2020) 100016.

[8] D. Devakumar and D.B. Jabaraj, Research on Gas Tungsten Arc Welding of Stainless Steel – An Overview, International journal of scientific & Engineering Research. 5 (2014) 7.

[9] M.R. Atma Raj and V.M. Joy Varghese, Determination of Distortion Developed During TIG welding of low carbon steel plate, International Journal of Engineering Research and General Science. 2 (2014).

[10] V.A. Rao and R. Deivanathan, Experimental investigation for welding aspects of stainless steel 310 for the process of TIG welding, Procedia Engineering. 97 (2014) 902–908.

[11] J. Joseph and S. Muthukumaran, Optimization of pulsed current GTAW process parameters for sintered hot forged AISI 4135 P/M steel welds by simulated annealing and genetic algorithm, Journal of Mechanical Science and Technology. 30 (2016) 145–155.

[12] K. Nandagopal and C. Kailasanathan, Analysis of mechanical properties and optimization of gas tungsten Arc welding (GTAW) parameters on dissimilar metal titanium (6Al4V) and aluminium 7075 by Taguchi and ANOVA techniques, Journal of Alloys and Compounds. 682 (2016) 503–516.

[13] R. Rudrapati, N. Chowdhury and A. Bandyopadhyay, Parametric optimization of TIG welding process in butt joining of mild steel and stainless steel, International Journal of Current Engineering and Technology. 6 (2016) 144–149.

[14] N. Kiaee and M. Aghaie-Khafri, Optimization of gas tungsten arc welding process by response surface methodology, Materials & Design (1980-2015). 54 (2014) 25–31.

[15] W. Chuaiphan and L. Srijaroenpramong, Effect of welding speed on microstructures, mechanical properties and corrosion behavior of GTA-welded AISI 201 stainless steel sheets, Journal of Materials Processing Technology. 214 (2014) 402–408.
[16] N. Choudhury, A. Bandyopadhyay and R. Rudrapati, Design optimization of process parameters for TIG welding based on Taguchi method, International Journal of Current Engineering and Technology. 2 (2014) 12–16.
[17] D.M. Arya, V. Chaturvedi and J. Vimal, Application of signal to noise ratio methodology for optimization of MIG welding process parameters, International Journal of Engineering Research and Applications. 3 (2013) 1904–1910.
[18] J. Wang, M. Lu, L. Zhang, W. Chang, L. Xu and L. Hu, Effect of welding process on the microstructure and properties of dissimilar weld joints between low alloy steel and duplex stainless steel, International Journal of Minerals, Metallurgy, and Materials. 19 (2012) 518–524.
[19] P. Kumar, K.P. Kolhe, S.J. Morey and C.K. Datta, Process parameters optimization of an aluminium alloy with pulsed gas tungsten arc welding (GTAW) using gas mixtures, Materials Sciences and Applications. 2 (2011) 251.
[20] P. Liu, Y. Li, H. Geng and J. Wang, Microstructure characteristics in TIG welded joint of Mg/Al dissimilar materials, Materials Letters. 61 (2007) 1288–1291.
[21] H.İ. Kurt and R. Samur, Study on microstructure, tensile test and hardness 304 stainless steel jointed by TIG welding, International Journal of Science and Technology. 2 (2013) 163–168.
[22] D. Simhachalam, N. Indraja and M.R. Roy, Experimental Evaluation of Mechanical Properties of Stainless Steel by TIG Welding at Weld Zone, International Journal of Engineering Trends and Technology (IJETT). 26 (2015).
[23] C.N. Patel and S. Chaudhary, Parametric optimization of weld strength of metal inert gas welding and tungsten inert gas welding by using analysis of variance and grey relational analysis, International Journal of Research in Modern Engineering and Emerging Technology. 1 (2013) 48–56.
[24] S. Naveenkumar, K. SooryaPrakash, G. Gokilakrishnan and N.V. Kamalesh, Parametric optimization of welding process of low carbon steel (AISI 1019) by using Taguchi's approach, International Journal For Technological Research In Engineering. 1 (2014) 415–425. http://ijtre.com/images/scripts/2014010705.pdf.
[25] S. Takhti, M. Reihanian and A. Ashrafi, Microstructure characterization and mechanical properties of gas tungsten arc welded cast A356 alloy, Transactions of Nonferrous Metals Society of China. 25 (2015) 2137–2146.
[26] K. Kishore, P.G. Krishna, K. Veladri and S.Q. Ali, Analysis of defects in gas shielded arc welding of AISI1040 steel using Taguchi method, ARPN Journal of Engineering and Applied Sciences. 5 (2010) 37–41.
[27] R. Sathish, B. Naveen, P. Nijanthan, K.A.V. Geethan and V.S. Rao, Weldability and process parameter optimization of dissimilar pipe joints using GTAW, International Journal of Engineering Research and Applications. 2 (2012) 2525–2530.
[28] B. Chandrakanth, S.V. Abinesh Kumar, S.A. Kumar and R. Sathish, Optimization and non-destructive test analysis of SS316L weldments using GTAW, Materials Research. 17 (2014) 190–195.
[29] P.K. Giridharan and N. Murugan, Optimization of pulsed GTA welding process parameters for the welding of AISI 304L stainless steel sheets, The International Journal of Advanced Manufacturing Technology. 40 (2009) 478–489.
[30] A.K. Hussain, A. Lateef, M. Javed and T. Pramesh, Influence of welding speed on tensile strength of welded joint in TIG welding process, International Journal of Applied Engineering Research. 1 (2010) 518.

[31] V. Gautam, Optimization of process parameters for Gas Tungsten Arc Welding of AA1100 Aluminium Alloy, International Journal of Current Engineering and Technology. 4 (2014) 788–792.
[32] L. Singh, R. Singh, N.K. Singh, D. Singh and P. Singh, An evaluation of TIG welding parametric influence on tensile strength of 5083 aluminium alloy, International Journal of Mechanical, Aerospace, Industrial, Mechatronic and Manufacturing Engineering. 7 (2013) 1262–1265.
[33] A.R. Rose, K. Manisekar, V. Balasubramanian and S. Rajakumar, Prediction and optimization of pulsed current tungsten inert gas welding parameters to attain maximum tensile strength in AZ61A magnesium alloy, Materials & Design. 37 (2012) 334–348.
[34] R. Sudhakaran, V. Vel-Murugan and P.S. Sivasakthivel, Effect of process parameters on depth of penetration in gas tungsten arc welded (GTAW) 202 grade stainless steel plates using response surface methodology, TJER. 9 (2012) 64–79.
[35] M.A. Ali, K. Ishfaq, M.H. Raza, M.U. Farooq, N.A. Mufti and C.I. Pruncu, Mechanical characterization of aged AA2026-AA2026 overcast joints fabricated by squeeze casting, The International Journal of Advanced Manufacturing Technology. 107 (2020) 3277–3297. https://doi.org/10.1007/s00170-020-05242-9.
[36] C. Akca and A. Karaaslan, Weldability of class 2 armor steel using gas tungsten arc welding, Archives of Materials Science and Engineering. 34 (2008) 110–112.
[37] B.K. Srivastava, S.P. Tewari and J. Prakash, A review on effect of preheating and/or post weld heat treatment (PWHT) on mechanical behavior of ferrous metals, International Journal of Engineering Science and Technology. 2 (2010) 625–631.
[38] Ş. Talaş, The assessment of carbon equivalent formulas in predicting the properties of steel weld metals, Materials & Design (1980-2015). 31 (2010) 2649–2653.
[39] M. Faghfouri, K. Ranjbar, R. Dehmolaei and A.H. Kaloorazi, Preventing Crack Formation at the Vicinity of the Fusion Zone in the Welding of Crane Rail Steel by Preheating Treatment, Metallography, Microstructure, and Analysis. 9 (2020) 541–552.
[40] E. Astm, Standard test methods for tension testing of metallic materials, Annual book of ASTM standards, in: ASTM, 2001.
[41] J.H. Jun, J.H. Park, M. Cheepu and S.M. Cho, Observation and analysis of metal transfer phenomena for high-current super-TIG welding process, Science and Technology of Welding and Joining. 25 (2020) 106–111.
[42] D.C. Montgomery, Design and analysis of experiments, John wiley & sons, 2017.
[43] M.U. Farooq, M.A. Ali, Y. He, A.M. Khan, C.I. Pruncu, M. Kashif, N. Ahmed and N. Asif, Curved profiles machining of Ti6Al4V alloy through WEDM: Investigations on geometrical errors, Journal of Materials Research and Technology. 9 (2020) 16186–16201.
[44] K. Ishfaq, M.U. Farooq, S. Anwar, M.A. Ali, S. Ahmad and A.M. El-Sherbeeny, A comprehensive investigation of geometrical accuracy errors during WEDM of Al6061-7.5%SiC composite, Materials and Manufacturing Processes. 36 (2020) 362–372. https://doi.org/10.1080/10426914.2020.1832683.
[45] H. Aglan and T. Rahman, Effect of Preheating Temperature and Cooling Rate on the Microstructure Development of Welded Pearlitic Rail Steel, Microscopy and Microanalysis. 26 (2020) 2662–2663. doi:10.1017/S1431927620022357.
[46] L. Wang, J. Chen and C. Wu, Numerical investigation on the effect of process parameters on arc and metal transfer in magnetically controlled gas metal arc welding, Vacuum. 177 (2020) 109391.
[47] T. Kasuya, N. Yurioka and M. Okumura, Methods for predicting maximum hardness of heat-affected zone and selecting necessary preheat temperature for steel welding, Nippon Steel Technical Report. (1995) 7–14.

[48] A. Ul-Hamid, H.M. Tawancy and N.M. Abbas, Failure of weld joints between carbon steel pipe and 304 stainless steel elbows, Engineering Failure Analysis. 12 (2005) 181–191.
[49] Q. Xue, D. Benson, M.A. Meyers, V.F. Nesterenko and E.A. Olevsky, Constitutive response of welded HSLA 100 steel, Materials Science and Engineering: A. 354 (2003) 166–179.
[50] R.S. Funderburk, Key Concepts in Welding Engineering, (1997) 2.
[51] R.S. Funderburk and P.W.H. Treatment, Welding Innovation Vol, XV, No 2. Post weld Heat Treatment. F. Lincoln Arc Welding Foundation. (1998).
[52] J.F. Lincoln, The procedure handbook of arc welding, The Lincoln Electric Company. (2000).
[53] K. Ishfaq, S. Anwar, M.A. Ali, M.H. Raza, M.U. Farooq, S. Ahmad, C.I. Pruncu and M. Saleh, B. Salah, Optimization of WEDM for precise machining of novel developed Al6061-7.5% SiC squeeze-casted composite, The International Journal of Advanced Manufacturing Technology. 111 (2020) 2031–2049. https://doi.org/10.1007/s00170-020-06218-5.